Conf-930701--6

LBL-33523
UC-402

Lawrence Berkeley Laboratory
UNIVERSITY OF CALIFORNIA

ENERGY & ENVIRONMENT DIVISION

To be presented at the Sixth International Conference on Indoor Air Quality and Climate, Helsinki, Finland, July 5–8, 1993, and to be published in the Proceedings

A Study of the Influence of a Gravel Subslab Layer on Radon Entry Rate Using Two Basement Structures

A.L. Robinson, R.G. Sextro, W.J. Fisk, K. Barbesi, J. Wooley, and H.A. Wollenberg

January 1993

ENERGY & ENVIRONMENT DIVISION

Prepared for the U.S. Department of Energy under Contract Number DE-AC03-76SF00098

To be Published in Proceedings of
Indoor Air '93, the 6th International
Conference on Indoor Air Quality
and Climate, July 5-8, 1993, Helsinki, Finland

LBL-33523

A STUDY OF THE INFLUENCE OF A GRAVEL SUBSLAB LAYER ON RADON ENTRY RATE USING TWO BASEMENT STRUCTURES

A.L. Robinson*, R.G. Sextro*, W.J. Fisk*, K. Garbesi*, J. Wooley*, and H.A. Wollenberg+

*Indoor Environment Program
Energy and Environment Program,
Lawrence Berkeley Laboratory
University of California, Berkeley, CA 94720

+Earth Sciences Division
Lawrence Berkeley Laboratory
University of California, Berkeley, CA 94720

January 1993

This work was supported by the Director, Office of Energy Research, Office of Health and Environmental Research, Environmental Sciences Division, and by the Assistant Secretary for Conservation and Renewable Energy, Office of Building and Community Systems, Building Systems and Materials Division of the U.S. Department of Energy, under Contract DE-AC03-76SF00098.

A STUDY OF THE INFLUENCE OF A GRAVEL SUBSLAB LAYER ON RADON ENTRY RATE USING TWO BASEMENT STRUCTURES

A.L. Robinson[1], R.G. Sextro[1], W.J. Fisk[1], K. Garbesi[1], J. Wooley[1], and H.A. Wollenberg[2]

[1]Energy and Environment Division, Lawrence Berkeley Laboratory, United States
[2]Earth Sciences Division, Lawrence Berkeley Laboratory, United States

ABSTRACT

In buildings with elevated radon concentrations, the dominant transport mechanism of radon is advective flow of soil gas into the building substructure. However, the building-soil system is often complex, making detailed studies of the radon source term difficult. In order to examine radon entry into buildings, we have constructed two room-size, precisely-fabricated basement structures at a site with relatively homogeneous, moderately permeable soil. The basements are identical except that one lies directly on native soil whereas the other lies on a high permeability aggregate layer.

The soil pressure field and radon entry rate have been measured for different basement pressures and environmental conditions. The subslab gravel layer greatly enhances the advective entry of radon into the structure; when the structures are depressurized, the radon entry rate into the structure with the subslab gravel layer is more than a factor of 3 times the radon entry rate into the other structure for the same depressurization. The gravel subslab layer also spreads the pressure field around the structure, extending the field of influence of the structure and the region from which it draws radon.

INTRODUCTION

Advective entry of soil gas is the dominant transport mechanism of radon in buildings with elevated radon concentrations. A number of different factors create the few pascal pressure differences between the building and its environment which drive advective soil gas flow: indoor outdoor temperature differences, wind, and imbalanced building ventilation systems.(1)

We have constructed two precisely-fabricated, highly-instrumented, room-sized basements in a well characterized, relatively homogeneous soil to examine radon entry into buildings. The structures are identical except for the presence of a high permeability gravel layer underneath one of the structures. Understanding the effect of a gravel subslab layer on the radon entry rate and pressure field provides valuable data for designing low-radon buildings and radon mitigation systems. This paper compares the radon entry rates into and the pressure fields around the two structures.

EXPERIMENTAL METHODS

We briefly describe important aspects of structure design, instrumentation, and site geology. Details of structure design and instrumentation are found in Fisk et al. (2). The structures are located on the top of wide flat ridge in the Santa Cruz Mountains near Ben Lomond, California. The rainfall at the site is approximately 150 cm per year, and is generally confined to the October-May period . The soil is a residual sandy loam, developed from quartz diorite, with a permeability of the order 10^{-11} m^2. Additional geological details for the site are found in Flexser et al. (3).

Both structures are identical except for the presence of a 12-cm-thick gravel layer underneath one of the structures. This structure is referred to as the west structure, and the structure with the native soil immediately below the slab is referred to as the east structure. Each structure is a single chamber with a floor dimension of 1.7 x 2.9 m and a height of 1.9 m (inside dimensions); only about 0.1 m of the walls extend above grade. Six smooth-walled slots, each 0.003 m wide and 1 m long, are installed in the floor of each structure to allow entry of soil gas into the structure through well-characterized openings. The slots simulate the shrinkage gap that occurs between footers and poured concrete floors. We have attempted to seal all other cracks between the structures and the surrounding soil to close off any uncharacterized soil gas entry points.

Each structure has 32 soil probes to measure pressure differences between the soil and the structure. Three sets of eight probes extend horizontally from the walls into the soil at depths of 0.18, 0.8, and 1.6 m below grade. These probes are referred to as high-wall, mid-wall, and low-wall probes respectively. There are three different lengths of horizontal sampling probes: 0.50, 1.71, and 2.39 m, measured from the outside of the wall to the middle of the sampling screen. The final eight probes extend vertically into the soil through the floor and are referred to as the subslab probes. There are five different lengths of subslab sampling probes: 0.24, 0.50, 1.11, 1.71, and 2.39 m, measured from the bottom of the slab to the middle of the sampling screen.

Continuous radon monitors (CRM) are used to measure the radon concentration of the air inside of the structure. The CRM data were interpreted using the method described by Thomas and Countess (5). An oscillating fan runs inside of each structure to ensure that the air inside of the structure is well mixed. Pressures are measured with high-sensitivity differential pressure transducers. Structure depressurization is maintained with an air pump and a computer-controlled mass-flow-controller.

Pressure Field:

The soil pressure field created by structure depressurization drives the advective soil gas entry into the structure . The pressure field quantifies the field of influence of the structure and provides detailed insight into advective soil-gas transport pathways. We describe the pressure field around a structure in terms of pressure coupling. Pressure coupling is the fraction of the total structure depressurization that is seen at a point in the soil. The total structure depressurization is the indoor-to-soil pressure difference measured with a floor-level, 5-m-long reference probe which extends into the soil beyond the structure's pressure field. We report pressure coupling rather than disturbance pressures because, assuming Darcy flow and negligible resistance of flow through the slots relative to the soil, the pressure coupling should be independent of structure depressurization. We compute the pressure coupling in the soil following the method described by Garbesi et al. (4). Pressure coupling experiments were run simultaneously in both structures in order to eliminate problems of changing environmental conditions such as soil moisture, temperature, and wind speed.

Radon Entry Rate:

Experiments were carried out to determine the steady-state radon entry rate into each structure at different structure depressurizations. These experiments were run for approximately two weeks to allow structure radon concentrations to reach their steady-state value.

The steady-state radon entry rate was computed using a simple steady-state mass balance

$$E = C(Q + \lambda V) \tag{1}$$

where E is the steady-state radon entry rate [Bq s^{-1}], Q is the flow rate of the exhaust flow from the structure [m^3 s^{-1}], C is the radon concentration of the air inside the structure [Bq m^{-3}], V is the volume of the structure [m^3], and λ is the radioactive decay constant of radon [s^{-1}].

The radon entry rate due to diffusion alone was determined by sealing the entry slots in each structure and running an experiment at neutral pressure, no imposed structure depressurization. The diffusive radon entry rates were then calculated by correcting the radon entry rate measured during a neutral pressure experiment for any measured structure depressurization due to environmental factors (wind, temperature differences, etc.) using the data for the radon entry rate as a function of structure depressurization described below.

RESULTS

Pressure coupling in the soil below the floor and adjacent to the structure walls ~1 m above the floor (mid-wall) is summarized in Figures 1 and 2, respectively. For each structure, these figures show both the pressure coupling measured in each of the eight subslab and mid-wall probes, and the average of the pressure coupling in probes of the same length (for example, the average value of the pressure coupling measured in the four east structure, 0.50-m-long, mid-wall probes). In Figures 1 and 2, the labels *Probe1, Probe2* ... identify the individual probes of a given length and the label *average* denotes the average value of the pressure coupling in the same length probes. The pressure coupling in the individual probes was calculated by averaging measurements, weighted by their uncertainties, made during several experiments run in July-September of 1992.

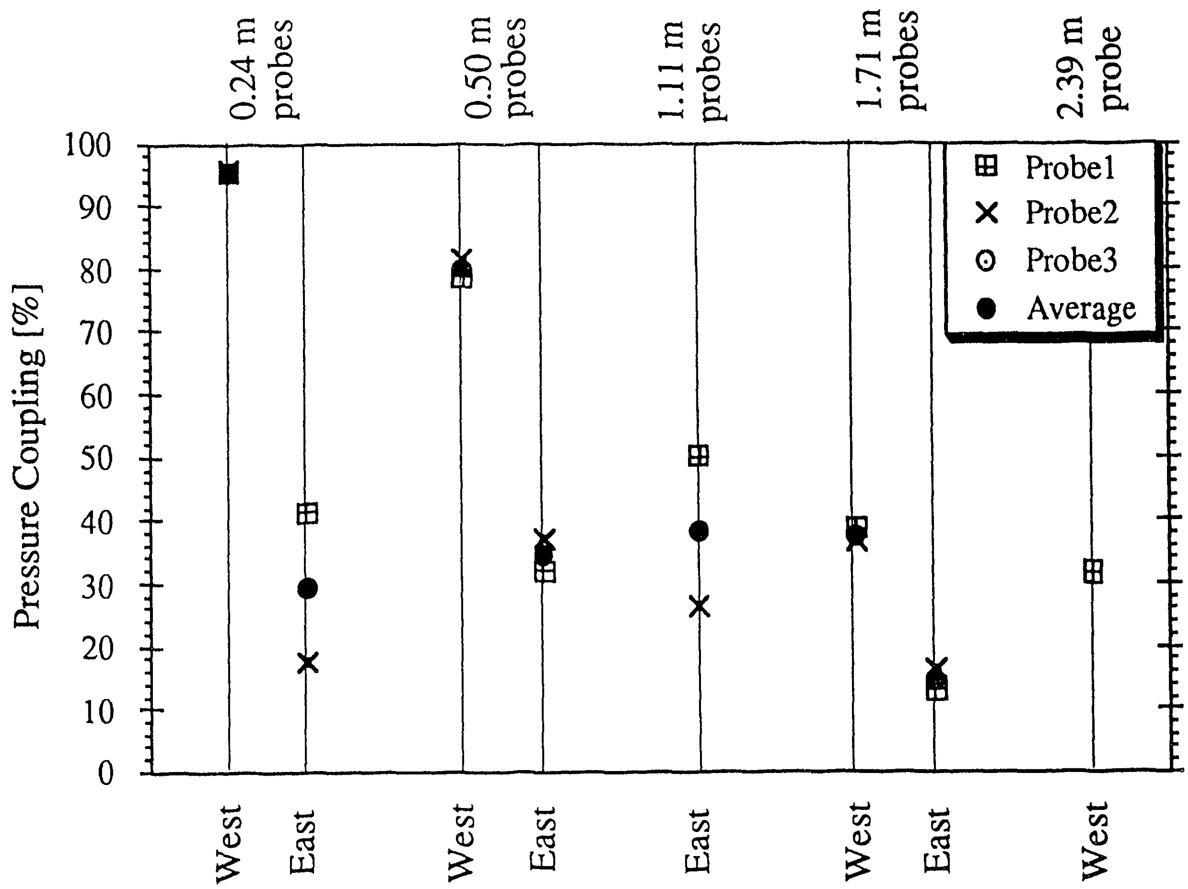

Fig 1. A comparison of east and west structure subslab pressure coupling. Uncertainties in pressure coupling are on the order of marker size. Note: there are no 1.11-m-long probes in the subslab region of the west structure, and no 2.39-m-long probes in the subslab region of the east structure.

A comparison of the pressure coupling measurements made around the east and west structures shows that the gravel subslab layer spreads the pressure field around the west structure. This expansion of the pressure field can be seen by comparing the pressure coupling in the east and west structure probes of the same length in the subslab and mid-wall regions. Beneath the west structure the pressure coupling in the 0.24 m subslab probes is more than a factor 3 greater than the pressure coupling in the corresponding east structure probes. The pressure coupling in the 1.71- and 2.39-m-long mid-wall probes of the west structure is 3 times larger than in the comparable east structure probes.

Another difference between the east and west structure pressure fields is the greater spatial uniformity of the pressure field around the west structure. The data in Figures 1 and 2 show that around the west structure the pressure coupling in the same length probes vary by less than 5% in the subslab, and by less than 30% in the mid-wall. In contrast, the pressure coupling in east structure 0.5 m mid-wall probes vary by a factory of 5, and the pressure coupling in the subslab 1.11 m probes vary by a factor of 2. The pressure coupling around the west structure also falls off smoothly as one moves further away from the structure. In contrast, beneath the east structure the pressure coupling is greater in the 1.11 m subslab probes than the 0.24 m subslab probes.

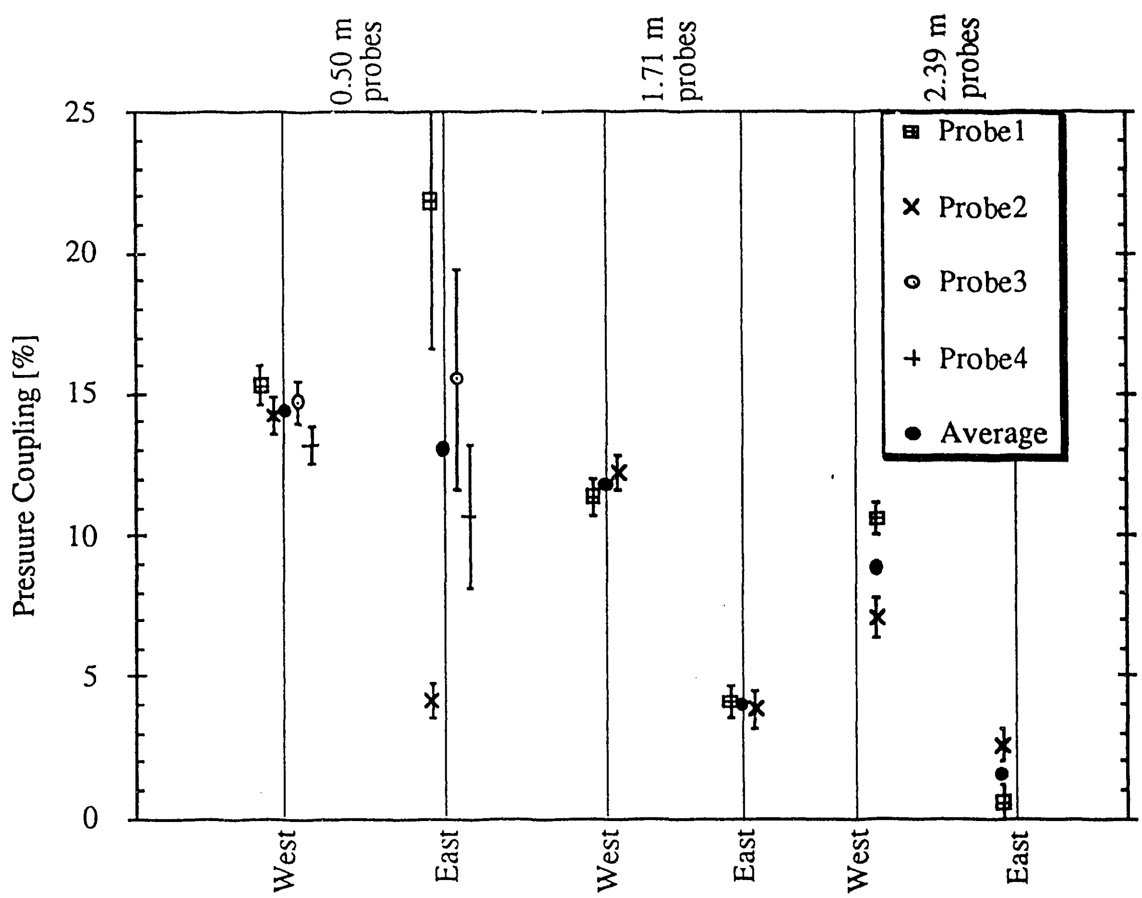

Fig 2. A comparison of east and west structure mid-wall pressure coupling (0.8 m below grade).

The steady-state radon entry rates as a function of structure depressurization are shown in Figure 3 for both the east and west structures. The lines in Figure 3 are from least squares fits to the radon entry rate vs. depressurization data. These regressions yield a steady-state radon entry rate of 0.78 Bq s^{-1} Pa^{-1} in the west structure and 0.23 Bq s^{-1} Pa^{-1} in the east structure. The observed steady-state radon entry rates due only to diffusion are essentially the same for both structures: 0.16 Bq s^{-1} into the west structure and 0.14 Bq s^{-1} into the east structure.

DISCUSSION

The results of our experiments directly demonstrate the dramatic effect that a subslab gravel layer has on the interaction between a building substructure and its soil environment. The gravel sublayer has two main effects: (1) it enlarges the field of influence of the structure, thereby increasing the volume of soil from which radon is drawn, and (2) it dramatically increases the radon entry rate into the structure.

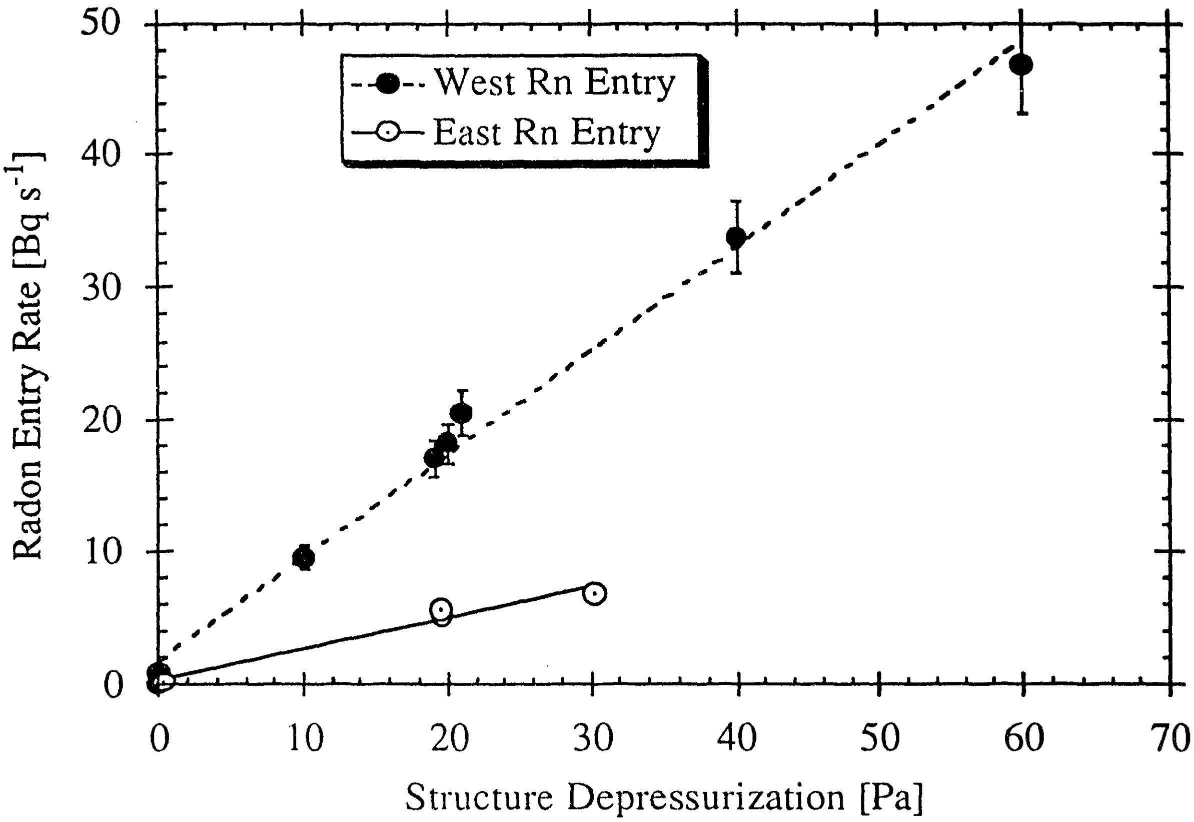

Fig 3. A comparison of east and west structure steady-state radon entry rates. East structure radon entry rate error and structure depressurization error are on the order of the marker size. The three west structure radon entry rate data points at 20 Pa are spread for clarity.

The 96% pressure coupling measured in the west structure 0.24 m subslab probes shows that the subslab gravel layer acts as a uniformly depressurized plenum beneath the west structure -- a large pressure sink at the same depressurization relative to the soil environment as the structure. In effect, the subslab gravel causes the west structure to act as if it has a dirt floor instead of a concrete floor with a few openings. In contrast, the approximately 30% pressure coupling measured in the east structure 0.24 m subslab probes shows that the pressure field quickly drops off below the east structure because it only communicates with the soil through six small openings. The subslab gravel causes the west structure to communicate with the soil environment through a much larger effective surface area than the east structure. This increased effective surface area causes both the expansion of the west structure's pressure field, and the dramatic increase in the advective entry of radon-laden soil gas into the west structure.

Local heterogeneities in soil properties cause spatial variation within the soil pressure field. For example, a high permeability pathway between a probe and a slot in the case of the east structure and a probe and the gravel layer in the case of the west structure will increase the pressure coupling of the soil at that probe. Assuming the soil conditions around the two structures are the same, the greater spatial variability of the east structure's pressure field shows that the east structure is much more affected by local soil heterogeneities than the west structure. This is because the east structure communicates with the surrounding soil environment through a much smaller area than the west structure. On the other hand, the gravel plenum underneath the west structure effectively smoothes over local heterogeneities by finding similar pathways to each probe.

The results of our experimental measurements of radon entry rate are consistent with a previous numerical model examination of the effect of different structural factors on radon entry into houses (6). That work predicted that a gravel subslab layer would increase the advective radon entry rate into a house by a factor of 5 when the soil permeability is less than 10^{-11} m^2. The permeability of the soil at the site where the structures are located is on the order of 10^{-11} m^2 (3).

Our radon entry measurements confirm that advective entry of radon is the dominant mode of radon entry into buildings, even at the few pascal pressure differences created by environmental factors. In addition, the presence of a gravel subslab layer appears to greatly increase the radon entry rate into a building substructure. Some radon mitigation strategies recommend the installation of a subslab gravel layer in new houses to allow more effective ventilation of substructure soil gas, should remedial measures be necessary (7). However, the enhanced radon entry rate due to the presence of the gravel layer could lead to an increased need for such mitigation systems.

ACKNOWLEDGMENTS

The authors would like to thank C. Khalizadeh and T. Nuzum for their technical assistance, and the California Department of Forestry and the Ben Lomond Nursery for their hospitality at the field site. This work was supported by the Director, Office of Energy Research, Office of Health and Environmental Research, Environmental Sciences Division, and by the Assistant Secretary for Conservation and Renewable Energy, Office of Building and Community Systems, Building Systems and Materials Division of the U.S. Department of Energy, under Contract DE-AC03-76SF00098.

REFERENCES

1. Nazaroff WW, Moed BA, Sextro RG. Soil as a source of indoor radon: generation, migration and entry. In: Nazaroff WW, Nero AV ed., Radon Decay Products in Indoor Air. New York: Wiley-Interscience, 1988:57-112.
2. Fisk WJ, Modera MP, Sextro RG et al. Radon entry into basements: approach, experimental structures, and instrumentation of the small structures research project. Lawrence Berkeley Laboratory, Berkeley, California, 1992:LBL-31864.
3. Flexser S, Wollenberg HA, Smith AR. Distribution of radon sources and its effect on radon emanation in granitic soil at Ben Lomond CA. Lawrence Berkeley Laboratory, Berkeley, California, 1992:LBL-31915.
4. Garbesi K, Sextro RG, Fisk WJ et al. Soil-gas entry into an experimental basement: model-measurement comparisons and seasonal effects. Environ. Sci. Technol. (in press).
5. Thomas JW, Countess RJ. Continuous radon monitor. Health Phys 1979;36:734-738.
6. Revzan KL, Fisk WJ. Modeling radon entry into houses with basements: the influence of structural factors. Indoor Air 1992;2:40-48.
7. Scott AG. Preventing radon entry. In: Nazaroff WW, Nero AV ed., Radon Decay Products in Indoor Air. New York: Wiley-Interscience, 1988:407-433.

END

DATE
FILMED
9 / 10 / 93